Involvement of neurogranin in the modulation of calcium/calmodulin-dependent protein kinase II, synaptic plasticity, and spatial learning: A study with knockout mice

Jhang Ho Pak*†‡, Freesia L. Huang*†, Junfa Li†, Detlef Balschun§, Klaus G. Reymann¶, Chin Chiang‖, Heiner Westphal**, and Kuo-Ping Huang†,††**

†Endocrinology and Reproduction Research Branch and **Laboratory of Mammalian Genes and Development, National Institute of Child Health and Human Development, National Institutes of Health, Bethesda, MD 20892; and §Department of Neurophysiology and ¶Project Group Neuropharmacology, Leibniz Institute for Neurobiology, D-39008 Magdeburg, Germany

Edited by Louis Sokoloff, National Institutes of Health, Bethesda, MD, and approved August 11, 2000 (received for review April 24, 2000)

Neurogranin/RC3 is a neural-specific Ca^{2+}-sensitive calmodulin (CaM)-binding protein whose CaM-binding affinity is modulated by phosphorylation and oxidation. Here we show that deletion of the Ng gene in mice did not result in obvious developmental or neuroanatomical abnormalities but caused an impairment of spatial learning and changes in hippocampal short- and long-term plasticity (paired-pulse depression, synaptic fatigue, long-term potentiation induction). These deficits were accompanied by a decreased basal level of the activated Ca^{2+}/CaM-dependent kinase II (CaMKII) ($\approx$60% of wild type). Furthermore, hippocampal slices of the mutant mice displayed a reduced ability to generate activated CaMKII after stimulation of protein phosphorylation and oxidation by treatments with okadaic acid and sodium nitroprusside, respectively. These results indicate a central role of Ng in the regulation of CaMKII activity with decisive influences on synaptic plasticity and spatial learning.

Neurogranin/RC3 (Ng) is a Ca^{2+}-sensitive calmodulin (CaM)-binding protein that is highly concentrated in selective neurons within the cerebral cortex, hippocampus, and striatum. This protein has been implicated in the regulation of numerous postsynaptic signal transduction pathways because of its role in the regulation of Ca^{2+} and CaM in neurons (1–3). The CaM-binding affinity of Ng is attenuated by phosphorylation with protein kinase C (PKC) and by oxidation with nitric oxide (NO) (4–7); both modifications have the potential to modulate neuronal free Ca^{2+} and CaM levels. The phosphorylated Ng also stimulates the G-protein-coupled phosphoinositide second messenger pathways that trigger the mobilization of Ca^{2+} from intracellular stores (8). PKC is the only known Ng kinase *in vitro* (5), and deletion of PKC γ gene in mice negates both the glutamate- and depolarization-mediated phosphorylation of Ng (9). The close functional relationship between Ng and PKC γ is further illustrated by their similar developmental expression patterns in the cerebral cortex (10–12). Previous studies also suggest that Ng plays a critical role in synaptic plasticity. Ng was found to become phosphorylated by PKC after induction of long-term potentiation (LTP), and the intracellular application of antibodies binding to the Ng phosphorylation site domain prevented the induction of LTP (13–15).

CaM-dependent kinase II (CaMKII), like Ng, is also highly concentrated in dendritic spines (1, 16) and the two proteins can be functionally related to each other. CaMKII has been proposed as a molecular decoder of Ca^{2+} spikes in neurons; it is also implicated in the modulation of gene expression, ion channel conductance, neurotransmission, and synaptic plasticity (17). Activation of CaMKII involves binding of Ca^{2+}/CaM to the regulatory domain to free the inhibition imposed by the autoinhibitory domain. The activated kinase can phosphorylate many substrates as well as its own autoinhibitory domain at Thr^{286} (αCaMKII). The autophosphorylated CaMKII remains partially active even in the absence of Ca^{2+}/CaM, which is referred to as autonomous activity (17). The autonomous CaMKII continues to propagate the autophosphorylation, a feature that has been implicated in associative learning in rodents and in hippocampal LTP (18, 19). In support of this hypothesis, mice lacking αCaMKII (20) or with mutation of the autophosphorylation site from Thr^{286} to alanine exhibited severe deficits in LTP and spatial learning (21).

We report here the generation of a strain of Ng knockout (KO) mice that did not exhibit obvious developmental and neuroanatomical abnormalities; however, these animals were profoundly impaired in spatial learning accompanied by changes in hippocampal short- and long-term plasticity. Our data suggest that the observed functional deficits of the KO mice are caused by the absence of Ng, which is crucial for a fine-tuned amplification of the Ca^{2+} signal and the activation of CaMKII.

Experimental Procedures

Generation and Characterization of Ng KO Mice. The use of animals was approved by the National Institute of Child Health and Human Development Animal Care and Use Committee. Mouse Ng genomic clones were isolated from λ FIX II genomic library (Stratagene) by using a labeled rat Ng cDNA as a probe. The sequence derived from two phage clones covered the 5′-flanking region, first exon and intron, and 54 bp of the second exon. A series of PCR were performed by using mouse genomic DNA as a template and primers corresponding to rat Ng genomic sequence (12) to obtain the entire genomic sequence of mouse Ng

This paper was submitted directly (Track II) to the PNAS office.

Abbreviations: Ng, neurogranin/RC3; CaM, calmodulin; PKC, protein kinase C; WT, wild type; KO, knockout; HET, heterozygote/heterozygous; CaMKII, calmodulin-dependent protein kinase II; Nm, neuromodulin/GAP-43; LTP, long-term potentiation; SNP, sodium nitroprusside; IPI, interpulse interval; PPD, paired-pulse depression; fEPSP, field excitatory postsynaptic potential; PPF, paired-pulse facilitation; X-gal, 5-bromo-4-chloro-3-indolyl β-D-galactoside.

Data deposition: The sequence reported in this paper has been deposited in the GenBank database (accession no. AF230869).

*J.H.P. and F.L.H. contributed equally to this work.

‡Present address: Institute for Environmental Medicine, University of Pennsylvania School of Medicine, Philadelphia, PA 19104.

‖Present address: Department of Cell Biology, Vanderbilt University Medical Center, Nashville, TN 37232.

††To whom reprint requests should be addressed. E-mail: kphuang@helix.nih.gov.

The publication costs of this article were defrayed in part by page charge payment. This article must therefore be hereby marked "*advertisement*" in accordance with 18 U.S.C. §1734 solely to indicate this fact.

Article published online before print: *Proc. Natl. Acad. Sci. USA*, 10.1073/pnas.210184697. Article and publication date are at www.pnas.org/cgi/doi/10.1073/pnas.210184697

(GenBank accession no. AF230869). To construct the targeting vector, the sequence coding for the first five amino acids in the first exon and the adjoining 98 bp of the first intron were replaced by bacterial *lacZ* and the neomycin resistance (*neo*) genes derived from pZINIMn vector. The targeting vector (linearized by *Not*I digestion) was transfected into embryonic stem cells derived from 129/sv mouse for homologous recombination, and clones obtained by the positive–negative selection strategy were positively identified by Southern blot (after *Sac*I digestion) with a probe containing 5′-flanking sequence. Two clones were used to generate chimeras. Germline transmission was obtained by crossing male chimeras with female C57BL/6 mice, and the F1 heterozygous (HET) littermates were then inbred to generate three genotypes. Genotyping was done by Southern blot of the *Sac*I-digested tail DNA by using ^{32}P-random primed probe (*Sac*I/*Bam*HI fragment) or by PCR with a 5′-primer (5′-AGAGTCGAGAGAAGGAGTTGGTCC-3′) and two 3′-primers, one corresponding to Ng (5′-CCACTTCCATCCCT-CACTCACCCC-3′, which was deleted in the targeting vector) and another one to *lacZ* sequence (5′-GAGTAACAAC-CCGTCGGATTCTCC-3′). In the Southern blot, the wild type (WT) has a positive band of 11.5 kb and the KO 6 kb and in the PCR assay, the WT has a band of 370 bp and the KO 780 bp. Polyclonal antibody (no. 270) against rat brain Ng (5) and an Ng-Ser^{36}-PO$_4$-specific antibody (no. 3615) were used for Western blot, and an Ng C-terminal peptide (66–78)-specific antibody (no. 2641) was used for immunocytochemical analysis. Antibodies for the detections of αCaMKII and autophosphorylated αCaMKII were obtained from Boehringer Mannheim and Promega, respectively. Frozen mouse brain sections fixed in 1% glutaraldehyde for 5 min were used for detection of the β-galactosidase activity.

Morris Water Maze Task. A circular pool (1.05 m in diameter) enclosed with white poster boards decorated with several symbols was filled with opaque water maintained at 25°C. Naive 3- to 8-mo-old mice received 3 blocks of 4 trials per day for 4 consecutive days to learn the position of a hidden platform (10 × 10 cm). A trial was started by lowering the animal into the water with head facing the wall at one of four starting positions, each located in a different quadrant of the pool. The trial was terminated if the animal found the platform or if 60 s had elapsed. During the trial, swim path and escape latency were recorded. Between trials, the mouse was allowed to sit on the platform for 15 s. At the end of the fourth day of training, a probe trial was conducted, i.e., each mouse was allowed to swim in the pool without platform for 60 s, and the time spent in each quadrant as well as the distance traveled were recorded. On the fifth day, the animals were given four blocks of the visible-platform task. In this version of the water maze, the platform was made visible (with a small grayish cylinder on top) and its position varied across trials.

Electrophysiology. Electrophysiological recordings were performed in the CA1 region of the hippocampal slices (400 μm). The slices were kept in a submerged-type chamber superfused with oxygenated artificial cerebrospinal fluid (ACSF) (in mM: NaCl 124/KCl 4.9/$MgSO_4$ 1.3/$CaCl_2$ 2.5/KH_2PO_4 1.2/$NaHCO_3$ 25.6/D-glucose 10) maintained at 33°C and allowed to recover for at least 2 h. A lacquer-coated stainless steel monopolar stimulation electrode and a glass recording electrode (filled with ACSF, 1–4 MΩ) were placed in the stratum radiatum of the CA1 region to record field excitatory postsynaptic potentials (fEPSPs). The initial slope of the fEPSP was used as a measure of this potential, thereby avoiding errors caused by a contamination by population spikes. After input/output curves were generated by recording fEPSP slopes at an increasing stimulation intensity, the stimulation voltage was adjusted to 35% of the maximum, and test stimuli were applied every 15 min. Once stable responses were obtained for 60 min, LTP was induced by a "strong" tetanization protocol consisting of 100 pulses at 100 Hz (double-pulse width), applied 3 times every 10 min. Experiments with mutant mice were interleaved with experiments with normal controls. To check paired-pulse facilitation (PPF), three paired pulses with interpulse intervals (IPIs) of 10, 40, 100, 200, and 500 ms were delivered at 60-s intervals at a stimulation voltage adjusted to 35% of the maximum. The three responses were averaged, and the degree of PPF was defined as % PPF (fEPSP slope of second pulse × 100/fEPSP slope of first pulse). Within-group comparisons were performed with the Wilcoxon matched-pairs signed rank test. Intergroup differences were analyzed by the Mann–Whitney *u* test and repeated measures by ANOVA.

Treatment of Hippocampal Slices and CaMKII Assay. Transverse hippocampal slices (400 μm) from adult mice were incubated in ACSF in a chamber saturated with 95%O_2/5%CO_2 at room temperature for at least 1 h before treatment. In each experiment, hippocampal slices from two WT and two KO mice were treated with 0.5 mM sodium nitroprusside (SNP) or 0.5 μM okadaic acid for the indicated time, and the tissues were kept frozen on dry ice after removing the medium. Each sample (8–10 slices) was homogenized in 0.12 ml of buffer (50 mM Tris·Cl, pH 7.8/2 mM EDTA/2 mM EGTA/5 mM Na pyrophosphate/50 mM KF/50 nM okadaic acid/0.5 mM sodium orthovanadate/5 μg/ml each of leupeptin, aprotinin, pepstatin A, and chymostatin/2 mM DTT/0.1% Nonidet P-40), centrifuged at 20,000 × *g* for 20 min and the supernatant used for protein determination, kinase activity assay, and immunoblot analysis. CaMKII activity was measured at 30°C for 3 min in a mixture (25 μl) containing 30 mM Hepes buffer (pH 7.6), 6 mM $MgCl_2$, 0.12 mM [γ-^{32}P]ATP, 1 mg/ml BSA, 2 mM EGTA, 4 mM DTT, 80 μM autocamtide-2, ± 1.2 μM CaM/2.4 mM $CaCl_2$, and 1 μg protein of tissue extract.

Results

Generation of Ng Mutant Mice. A targeting vector containing *lacZ* and *neo* genes was used for homologous recombination in embryonic stem cells (Fig. 1*A*). Approximately 20% of the selected embryonic stem cell clones harbored the disrupted Ng gene. Two separate clones were used to generate chimeric mice. Male chimeras were bred with C57BL/6 female to produce HET that were subsequently inbred to produce WT, HET, and KO progeny at a ratio expected for the segregation of a nonlethal mutation (1:2:1). These genotypes were identified by either Southern blot (Fig. 1*B*) or PCR (Fig. 1*C*). Northern blot (Fig. 1*D*) and Western blot (Fig. 1*E*) confirmed that the KO mice did not produce Ng mRNA or Ng protein. As indicated by immunoblotting with the polyclonal antibody no. 270, which detects both Ng and neuromodulin/GAP-43 (Nm) (Fig. 1*E*), the hippocampal and cortical Ng levels of the HET mice were approximately one-half of those in WT mice. In contrast, Nm was present in comparable levels in all three genotypes.

Mutant mice appeared to have normal growth, motor coordination, and longevity. No detectable gross anatomical abnormalities in the KO mice were seen in the hippocampus, neocortex, olfactory bulb, and striatum by light microscopy of cresyl violet-stained sections or those stained with Nm or CaM antibodies (data not shown). The KO mice were devoid of Ng immunoreactivity throughout all brain sections examined. Strong positive 5-bromo-4-chloro-3-indolyl β-D-galactoside (X-gal) staining in the KO mice was seen in layers II–IV and layer VI of the cerebral cortex, cortical amygdaloid nucleus, and hippocampus. These staining patterns exhibited good correspondence with the Ng-positive staining in WT mice (Fig. 2),

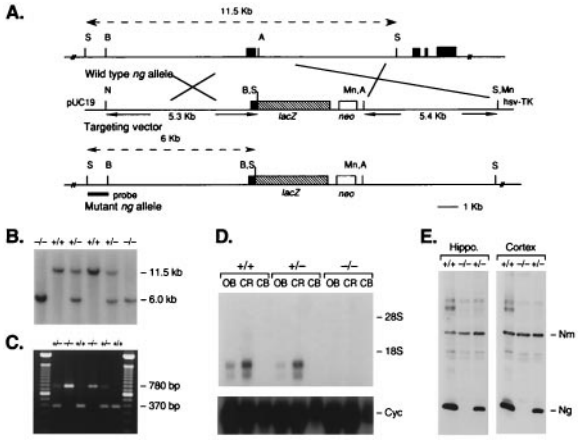

Fig. 1. Generation of Ng KO mice. (*A*) Restriction map of the native and mutant Ng alleles and targeting vector. The locations of the Ng gene exon (solid block), herpes simplex virus thymidine kinase gene (hsv-TK), neomycin resistance gene (*neo*), *lacZ* gene, and the probe for Southern blot analysis to identify the various genotypes are shown. (*B*) Southern blot analysis of *Sac*I-digested genomic DNA from mouse tails. (*C*) PCR analysis of the tail DNA for routine genotyping. (*D*) Northern blot analysis of Ng mRNA derived from olfactory bulb (OB), cerebral cortex (CR), and cerebellum (CB). Approximately 20 μg of RNA from each tissue was analyzed by using labeled rat Ng cDNA as a probe and referenced with signal probed with cyclophilin (cyc) cDNA. (*E*) Immunoblot analysis of Ng and Nm in tissue extracts derived from hippocampus and cerebral cortex. The polyclonal antibody (no. 270) detects both Ng and Nm.

suggesting that the expression of *lacZ* gene is under the control of the Ng promoter.

Ng KO Mice Exhibit Deficits in Learning and Memory. Three sets of mice (n = 40, 43, and 39 for WT, HET, and KO, respectively) were examined for their performances in the hidden platform, visible platform, and probe trial versions of the Morris water maze. After 4 consecutive days of training, all 3 sets of mice showed a significant decrease in their escape latencies (Fig. 3*A*). The escape latencies of the WT, HET, and KO mice at the fourth day of training (block 10–12) were 10.4 ± 0.75, 15.4 ± 1.2, and 25.9 ± 1.4 s, respectively, and ranks of performance were WT>HET>KO (Kruskal–Wallis ANOVA, H = 89.9, $P \leq$ 0.001). After the hidden platform test, all three sets of mice performed equally well in their visible platform tests, indicating

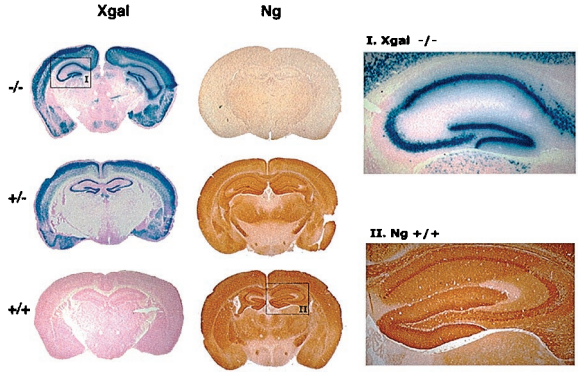

Fig. 2. Staining of the mouse brain sections with X-gal and Ng-specific antibody. Coronal sections through the hippocampus of the WT (+/+), HET (+/−), and KO (−/−) mice were stained with X-gal or with Ng-specific antibody (no. 2641). The magnified areas show a good correspondence between the X-gal and Ng-positive staining of neurons between +/+ and −/− mice. X-gal staining is restricted to neuronal cell bodies, whereas Ng-positive staining covers both cell bodies and processes.

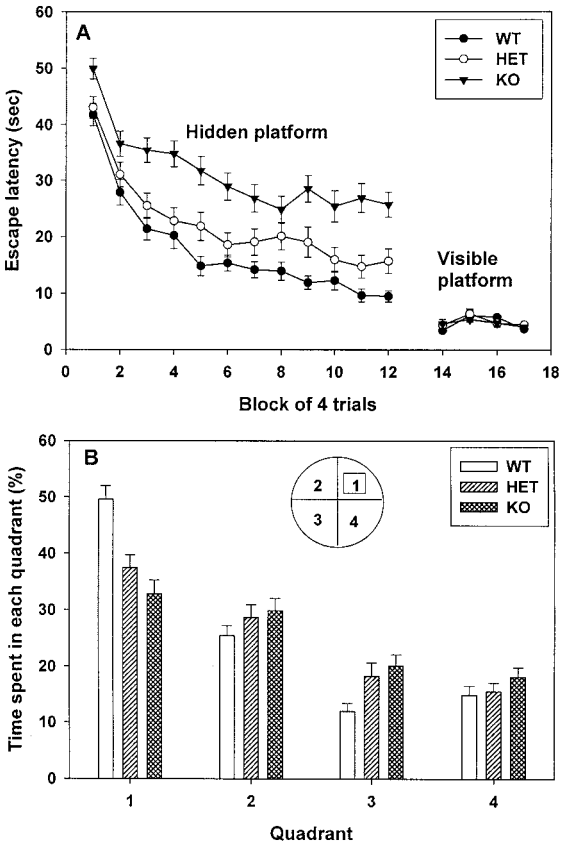

Fig. 3. Learning performance in the Morris water maze. (*A*) In the first part of the experiment, WT (+/+, n = 40), HET (+/−, n = 43), and KO (−/−, n = 39) mice received 12 blocks of training (3 blocks of 4 trials per day for 4 consecutive days) in the hidden platform version of the maze. The graph shows the escape latency to find the hidden platform for each genotype over successive blocks of trial. Thereafter, each animal was given 4 blocks of the visible platform test (n = 18, 18, and 20 for WT, HET, and KO, respectively). (*B*) During the probe trial after the twelfth block of training, WT mice spent significantly more time at the trained quadrant no. 1 (49.5 ± 2.4%, n = 40) than did KO mice (32.8 ± 2.4%, n = 39), and HET mice displayed an intermediate performance (37.4 ± 2.2%, n = 43) (one-way ANOVA, $P < 0.001$). Means ± SEM are given.

their differences in the hidden platform tests were not because of impairment in their vision, swimming ability, or motivation. After the fourth day of training, mice were subjected to probe trials to test their spatial memories without the hidden platform. The WT mice spent 49.5 ± 2.4% of the time swimming at the target quadrant as compared with 37.4 ± 2.2 for the HET and 32.8 ± 2.4 for the KO mice (Fig. 3*B*); the differences between the three genotypes were statistically significant (one-way ANOVA, $P < 0.001$). Interestingly, the performances of the HET mice were intermediate between the WT and KO mice, which apparently correlated with the hippocampal Ng levels. The HET mice attained 62.6 ± 9.1% (SD, n = 15) of the WT values (by quantitative Western blot analysis), and the KO contained no Ng. In accordance with the findings in the water maze, the KO mice also exhibited a similar performance decline in contextual fear conditioning [T. Miyakawa, J.H.P., F.L.H., K.-P.H. & J. N. Crawley (1999) *Society of Neuroscience Meeting Abstract* **257,** 13], another hippocampus-dependent learning paradigm.

Deletion of Ng Causes Changes in the Induction of Hippocampal LTP and in Short-Term Plasticity. Although both the WT and KO mice expressed LTP with a repeated strong tetanization protocol (3 ×

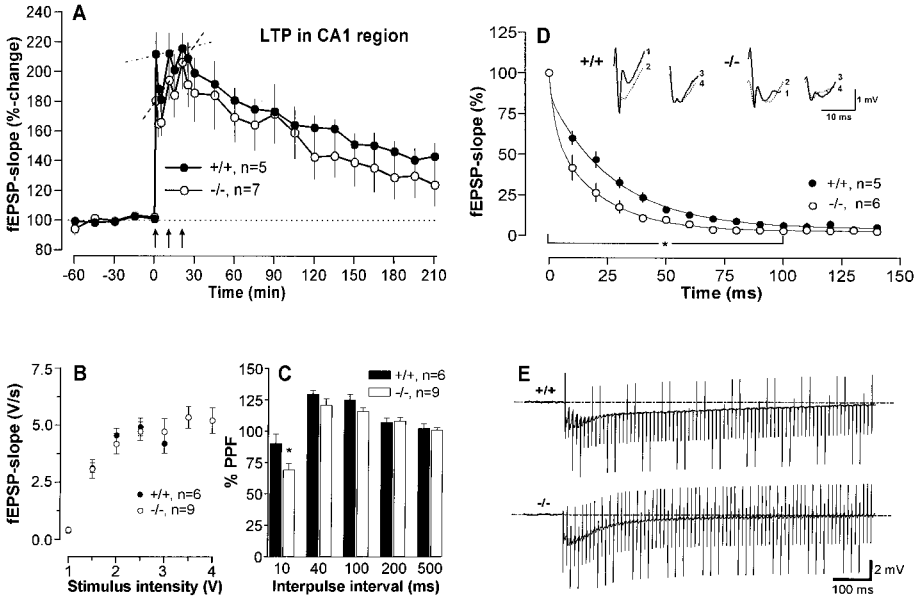

Fig. 4. LTP, basal synaptic transmission, and short-term plasticity in the hippocampal CA1 region of WT and KO mice. (*A*) LTP was induced by a repeated strong tetanization protocol consisting of 3 stimulus trains at 100 Hz (0.2 msec per polarity) with a 10-min intertrain interval. During the initial phase of potentiation, WT mice attained nearly the maximal level of potentiation after the first tetanus, whereas KO mice progressively increased the potentiation after each tetanus. For KO (but not WT) mice, the magnitude of the third tetanus potentiation was significantly greater than that of the first ($P = 0.018$ Wilcoxon matched-pairs signed rank test). Arrows indicate the time of tetanization. (*B*) Input/output curves of the KO and WT mice. fEPSP slopes were recorded at increasing stimulation intensities until a maximum was attained. There were no significant differences between the two groups. (*C*) Short-term plasticity as evaluated by paired-pulse stimulation at different IPIs. Although paired-pulse stimulation at an IPI of 10 ms resulted in PPD, at all other IPIs, PPF appeared. Note the stronger PPD of KO mice ($P < 0.05$). (*D*) Decay of fEPSPs during the first tetanic stimulation. The slope of 15 consecutive fEPSPs immediately at the onset of tetanic stimulation was determined, averaged across each group, and plotted vs. time. The curves were obtained by nonlinear fits with a two-phase exponential equation. The fEPSPs of KO mice decayed much faster than the WT in the initial part (first 100 ms) of the decay ($P = 0.022$, ANOVA with repeated measures). *Insets* show analogue traces of the first four fEPSPs during the first tetanization. Note the marked decay of fEPSP slope of the KO mouse between the first and second recording. (*E*) Representative analogue recordings of fEPSP changes in a WT vs. KO during the first tetanization. The faster decay of fEPSPs in the KO results in a smaller depolarizing envelope evoked by summation of the fEPSPs (area: WT, 878.4 units; KO, 530.5 units). The applied sampling rate permits a clear distinction of the fEPSPs between the WT and KO.

100 Hz, 1 s, 10-min interval) that lasted for more than 3 h (Fig. 4*A*), there was a difference in the induction of potentiation. The WT mice attained a near maximal level of potentiation after the first tetanus, whereas the KO mice started from a lower level, and every additional tetanization added another portion to potentiation. As a consequence, there is a statistically significant difference in the level of potentiation between the first and third tetanus in the KO but not in the WT mice ($P = 0.018$, Wilcoxon matched-pairs signed rank test). The differences in LTP induction were not caused by changes in basal synaptic function, as evidenced by input/output (I/O) curves (Fig. 4*B*), which showed only a tendency of both the WT and KO mice to attain the maximum of the I/O curve at higher stimulation intensities.

We next examined whether short-term plasticity was affected by deletion of Ng. A common form of short-term plasticity is observed when two identical stimuli are delivered to homosynaptic afferent fibers in rapid succession (a conditioning stimulus followed by a test stimulus). Depending on the IPI, this procedure results in either depression or facilitation of the test stimulus (22). At IPIs $\geq$ 40 ms, PPF was observed with no detectable differences between the KO and WT mice (Fig. 4*C*). In contrast, at an IPI of 10 ms, both strains displayed paired-pulse depression (PPD), which was significantly more so in the KO as compared with their WT littermates ($P \leq 0.05$). The higher magnitude of depression of KO mice at 10 ms tempted us to check whether this might result in different tetanization kinetics because the same IPI was contained in the tetanic stimulation at 100 Hz. To estimate the decaying kinetics of fEPSP during tetanization, the slope of the first 15 consecutive fEPSPs during each tetanic stimulation was determined, averaged across each strain of mice, and plotted vs. time. As depicted in Fig. 4*D* for the first of three successive tetanic stimulations, the recorded fEPSPs of each strain displayed a rapid exponential decline that is significantly better fitted by a two-phase exponential equation ($y = a^*e^{-t/\tau 1} + b^*e^{-t/\tau 2} + c$) as compared with a one-phase exponential decay ($P < 0.01$). It is evident from the graph that the fEPSPs of KO mice decayed much faster during the initial phase of tetanic stimulation, which is supported by their respective time constants of the slow components of 21.0 ms in the KO and 27.7 ms in the WT. Thus, the decay curves of the WT and KO mice are significantly different during the initial 100 ms (Fig. 4*D*, $P = 0.022$, ANOVA with repeated measurements). A slightly smaller strain difference was discernible in the decline of fEPSPs during the second and third tetanic stimulations (data not shown). The faster decay of fEPSPs in KO mice was accompanied by a smaller depolarizing envelope evoked by summation of the fEPSPs as an example given in Fig. 4*E*.

Ng KO Mice Have a Defective Mechanism for the Activation of CaMKII. In search of biochemical correlates of the behavioral and electrophysiological changes in the KO mice, CaMKII activities in hippocampal extracts were measured. The total hippocampal CaMKII activity in the KO mice was $\approx$15% higher than that of the WT (97.7 $\pm$ 4.03 vs. 84.5 $\pm$ 3.35 nmol/min/mg, $n = 16$, t test, $P < 0.05$), whereas the autonomous activity in the KO was $\approx$60% that of the WT mice (5.92 $\pm$ 0.46 vs. 8.93 $\pm$ 0.66 nmol/min/mg, $n = 16$, t test, $P < 0.001$). The percent of autonomous activity in the WT was 1.75-fold greater than that of the KO (10.5 $\pm$ 0.54

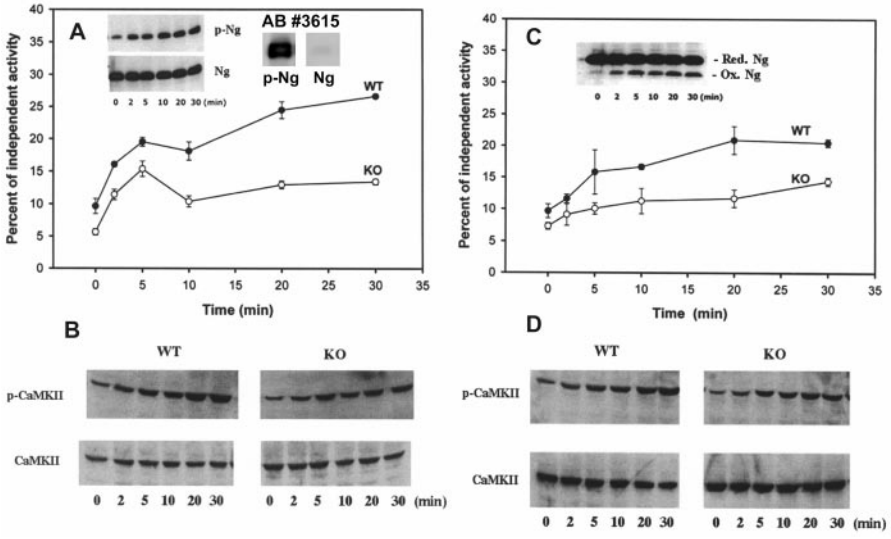

Fig. 5. Okadaic acid- and SNP-induced modifications of Ng and activation of CaMKII. Hippocampal slices from WT and KO mice were incubated with 0.5 μM of okadaic acid (*A* and *B*) or 0.5 mM SNP (*C* and *D*). At timed intervals, samples were taken and tissue extracts used for the measurement of CaMKII activity in the presence or absence of Ca^{2+}/CaM. Percent of Ca^{2+}/CaM-independent activity was determined. A PO_4-Ng antibody (antibody no. 3615), which is specific for the phosphorylated form, was used for the detection of p-Ng (*A Inset*) and antibody no. 270 for the detection of total Ng (*A Inset*) and the reduced (Red) and oxidized (Ox) forms (*C Inset*). For determination of Ng oxidation (*C Inset*), slices were homogenized in buffer containing 100 mM iodoacetamide without DTT and electrophoresis carried out under nonreducing condition to preserve the extent of oxidation. Autophosphorylated (p-CaMKII) and total αCaMKII were determined by using commercially available antibodies (*B* and *D*). The increase in autophosphorylated CaMKII corresponds well with the increase in the Ca^{2+}/CaM-independent activity. The data represent the mean ($\pm$ SEM) of three separate experiments by using slices from six each of the WT and KO mice.

vs. $6.0 \pm 0.36\%, n = 16$, *t* test, $P < 0.001$), suggesting the KO mice contain less autophosphorylated CaMKII than that of the WT. This was also confirmed by quantitative immunoblot analysis with αCaMKII-Thr^{286}-PO_4-specific antibody, with which the KO was found to be $49.5 \pm 13\%$ ($n = 4$) of the level of the WT.

To investigate further whether CaMKII autophosphorylation in the KO mice is defective, hippocampal slices were treated with chemicals known to increase protein phosphorylation or oxidation. Treatment of the hippocampal slices with okadaic acid (0.5 μM), which caused Ng phosphorylation in the WT (Fig. 5*A Inset*), resulted in a larger increase in the autonomous kinase activity of the WT as compared with that of the KO mice (Fig. 5*A*). The increase in the autonomous CaMKII activity corresponded with the autophosphorylation at Thr^{286} of αCaMKII determined by immunoblot with αCaMKII-Thr^{286}-PO_4-specific antibody (Fig. 5*B*). Okadaic acid caused a biphasic increase in the autonomous CaMKII in both the WT and KO mice. The initial rate of increase was similar for both, but the second phase of increase was greater in WT than in KO mice. After 30 min of incubation, the Ca^{2+}/CaM-independent activities in the WT and KO were 26.6 ± 0.3 vs. $13.4 \pm 0.4\%$ ($P < 0.001$). Incubation of the hippocampal slices with SNP (0.5 mM), which caused Ng oxidation in the WT (Fig. 5*C Inset*), also resulted in a larger increase in autonomous CaMKII activity (20.2 ± 0.4 in WT vs. $13.2 \pm 1.2\%$ in KO after 30 min, $P < 0.01$) (Fig. 5*C*) and autophosphorylation at Thr^{286} (Fig. 5*D*) in the WT than the KO mice. The consistently higher level of CaMKII autophosphorylation in the WT slices as compared with that of the KO indicates a critical role of Ng in the generation of autonomous CaMKII.

Discussion

Ng is a postsynaptic protein believed to be involved in the regulation of intracellular Ca^{2+} and CaM levels after neuronal excitation. As Ca^{2+}/CaM play a central role in controlling a plethora of cellular events, deletion of Ng could affect multifarious signaling pathways. In the adult mouse brain, Ng is expressed at high levels in the neocortex, hippocampus, and amygdala, brain areas known to be important for learning and memory in vertebrates. Indeed, the Ng KO mice, which express no Ng in the hippocampus, exhibited severe performance deficits in the Morris water maze, a hippocampus-dependent spatial learning paradigm. In addition to these learning deficits, Ng KO mice displayed changes in hippocampal short- and long-term plasticity as well as a defective mechanism for the activation of CaMKII. The phenotypic changes in the Ng KO mice resemble in certain respects those of the αCaMKII KO and the autophosphorylation site-defective mutants (20, 21). This perhaps is expected, as Ng functions as an upstream modulator for many neuronal signaling pathways, including those using Ca^{2+}, CaM, cyclic nucleotides, and NO. Thus, the Ng KO mouse will be a very useful genetic model to delineate the roles of these messengers in synaptic plasticity.

Paired-pulse stimulation, a widely used protocol for the investigation of short-term plasticity, evoked a greater PPD at an IPI of 10 ms in KO mice as compared with controls. At IPIs $\geq$ 40 ms, both strains displayed EPSP facilitation (PPF), which agreed with other studies (23). The PPD obtained at an IPI of 10 ms is most likely because the second pulse arrives during the period of recurrent $GABA_A$-mediated inhibition generated by the conditioning stimulus (23). This inhibition overrides facilitatory effects because of short-term presynaptic enhancement (24, 25). Because of a stronger PPD at 10 ms, KO mice displayed a faster decay of fEPSPs during tetanization at 100 Hz, which contains the same IPI. However, during long trains of repetitive stimulation at high frequencies, the $GABA_A$-mediated inhibition shows a rapid rundown (26). Therefore, this inhibition might play a role during the initial phase of tetanization, but the observed depression of fEPSPs over time is predominantly because of a presynaptic phenomenon termed synaptic fatigue. This form of short-term synaptic depression can be largely attributed to rapid depletion of a readily releasable pool of vesicles (27, 28). $GABA_A$-mediated inhibition and synaptic fatigue represent the principal sources of the observed rapid decline of fEPSPs during tetanization. The faster decay in KO

mice will result in a smaller depolarizing envelope evoked by summation of the fEPSPs (29), which in turn is likely to be responsible for the reduction of the initial magnitude of potentiation to about 65% of that of the WT. This difference was stepwise reduced by the two subsequent tetanic stimulations, which resulted in a similar LTP maintenance for both the WT and KO mice. It is difficult to deduce whether the lower initial potentiation resulted from deficits in posttetanic potentiation or LTP. The apparent changes of GABAergic inhibition and the presumably postsynaptic expression of functional disturbances after Ng deletion strongly suggest a deteriorated interaction between interneurons and pyramidal cells in the hippocampal CA1 region of the KO mice. These alterations are likely to result in shifted computational properties of hippocampal networks.

Our biochemical data indicate that the observed deficits in hippocampal synaptic plasticity and hippocampus-dependent spatial learning of the KO mice could be because of an aberrant regulation of neuronal Ca^{2+} and CaM levels, which affect the activation of many Ca^{2+}/CaM-dependent enzymes. Indeed, in mutant mice, the basal level of the activated CaMKII was reduced to about 60% of the WT values, and the mechanism for the stimulation of CaMKII autophosphorylation in the hippocampus was impaired. Reduction of the neuronal level of the activated CaMKII is likely to have a decisive impact on downstream signaling, such as the phosphorylations of SynGap, mitogen-activated protein kinases, and cAMP-responsive element-binding protein, thought to be important for the consolidation and formation of long-term memory (30, 31). Furthermore, phosphorylation of the GluR1 subunit of the AMPA receptor by the activated CaMKII (32) leads to an enhanced receptor channel conductance (33), which plays a major role in mediating the postsynaptic mechanism of LTP. A deficit in the activation of CaMKII in the Ng KO mice could dampen the increase of AMPA channel conductance during LTP induction and magnify the responses to GABAergic inhibition.

Because the phosphorylation and oxidation of Ng with okadaic acid and SNP, respectively, provide a greater boost of CaMKII autophosphorylation in the WT mice than that of the mutants, we conclude that these modified forms of Ng participate in the regulation of CaMKII autophosphorylation. In this respect, one may consider that CaM sequesters Ng at the basal level of $[Ca^{2+}]_i$ and release it on a rise in $[Ca^{2+}]_i$, so it can be activated via phosphorylation by PKC or oxidation by NO. As Ng is enriched in the dendritic spines (1), it may concentrate CaM there for localized responses on Ca^{2+} influx triggered by glutamate release and/or depolarization. Thus, at basal levels of $[Ca^{2+}]_i$, Ng and CaM can be considered as mutual silencers, i.e., CaM prevents Ng from being phosphorylated or oxidized, and Ng dampens the sensitivity of CaM to minor fluctuations of $[Ca^{2+}]_i$. When $[Ca^{2+}]_i$ exceeds a certain threshold, Ca^{2+}/CaM enhance Ng oxidation by stimulation of NO synthase, and Ca^{2+} stimulates PKC to phosphorylate Ng. The phosphorylated and oxidized Ng in turn may support an elevation of the Ca^{2+}/CaM concentration. Taken together, the data obtained with the Ng KO mice support the hypothesis that Ng and CaM maintain a distinct functional interaction, which is essential for a fine-tuned amplification of the Ca^{2+} signal. Any disturbance of this unique partnership will lead to detrimental consequences in important neural function such as synaptic plasticity and learning and memory.

We thank Drs. Jacqueline N. Crawley and Theresa C. Gleason for advising us on the behavioral study, Dr. Anthony Wynshaw-Boris for use of the Morris water maze, Drs. Eric Lee and Alex Grinberg, Mrs. Sing-Ping Huang, and Mr. Daniel Abebe for help in generation and upkeep of the neurogranin knockout mice, and Ms. Katrin Böhm for excellent technical assistance in the electrophysiological study.

1. Gerendasy, D. D. & Sutcliffe, J. G. (1997) *Mol. Neurobiol.* **15,** 131–163.
2. Prichard, L., Deloulme, J. C. & Storm, D. R. (1999) *J. Biol. Chem.* **274,** 7689–7694.
3. Chakravarthy, B., Morley, P. & Whitfield, J. (1999) *Trends Neurosci.* **22,** 12–16.
4. Baudier, J., Deloulme, J. C., VanDorsselaer, A. V., Black, D. & Matthes, H. W. D. (1991) *J. Biol. Chem.* **266,** 229–237.
5. Huang, K.-P., Huang, F. L. & Chen, H.-C. (1993) *Arch. Biochem. Biophys.* **305,** 570–580.
6. Sheu, F.-S., Mahoney, C. W., Seki, K. & Huang, K.-P. (1996) *J. Biol. Chem.* **271,** 22407–22413.
7. Li, J., Pak, J. H., Huang, F. L. & Huang, K.-P. (1999) *J. Biol. Chem.* **274,** 1294–1300.
8. Cohen, R. W., Margulies, J. E., Coulter, P. M., II & Watson, J. B. (1993) *Brain Res.* **627,** 147–152.
9. Ramakers, G. M. J., Gerendasy, D. D. & de Graan, P. N. E. (1999) *J. Biol. Chem.* **274,** 1873–1874.
10. Watson, J. B., Battenberg, E. F., Wong, K. K., Bloom, F. E. & Sutcliffe, J. G. (1990) *J. Neurosci. Res.* **26,** 397–408.
11. Huang, F. L., Yoshida, Y., Nakabayashi, H., Young, W. S., III & Huang, K.-P. (1988) *J. Neurosci.* **8,** 4734–4744.
12. Sato, T., Xiao, D.-M., Li, H., Huang, F. L. & Huang, K.-P. (1995) *J. Biol. Chem.* **270,** 10314–10322.
13. Klann, E., Chen, S.-J. & Sweatt, J. D. (1992) *J. Neurochem.* **58,** 1576–1597.
14. Ramakers, G. M. J., De Graan, P. N. E., Urban, I. J. A., Kraay, D., Tang, T., Pasinelli, P., Oestreicher, A. B. & Gispen, W. H. (1995) *J. Biol. Chem.* **270,** 13892–13898.
15. Fedorov, N. B., Pasinelli, P., Oestricher, A. B., De Graan, P. N. E. & Reymann, K. G. (1995) *Eur. J. Neurosci.* **7,** 819–822.
16. Kennedy, M. B. (1998) *Brain Res. Rev* **26,** 243–257.
17. Braun, A. P. & Schulman, H. (1995) *Annu. Rev. Physiol.* **57,** 417–445.
18. Lisman, J. (1994) *Trends Neurosci.* **17,** 406–412.
19. Nicoll, R. A. & Malenka, R. C. (1995) *Nature (London)* **377,** 115–118.
20. Silva, A. J., Stevens, C. F., Tonegawa, S. & Wang, Y. (1992) *Science* **257,** 201–206.
21. Giese, K. P., Fedorov, N. B., Filipkowski, R. K. & Silva, A. J. (1998) *Science* **279,** 870–873.
22. Zucker, R. S. (1989) *Annu. Rev. Neurosci.* **12,** 13–31.
23. Creager, R., Dunwiddie, T. & Lynch, G. (1980) *J. Physiol. (London)* **299,** 409–424.
24. Fisher, S. A., Fischer, T. M. & Carew, T. J. (1997) *Trends Neurosci.* **20,** 170–177.
25. Katz, B. & Miledi, R. (1968) *J. Physiol. (London)* **195,** 481–492.
26. Davies, C. H. & Collingridge, G. L. (1993) *J. Physiol. (London)* **472,** 245–265.
27. Dobrunz, L. E. & Stevens, C. F. (1997) *Neuron* **18,** 995–1008.
28. Wang, L.-Y. & Kaczmarek, L. K. (1998) *Nature (London)* **394,** 384–388.
29. Davies, C. H. & Collingridge, G. L. (1993) *J. Physiol. (London)* **472,** 245–265.
30. Chen, H.-J., Rojas-Soto, M., Oguni, A. & Kennedy, M. B. (1998) *Neuron* **20,** 895–904.
31. Impey, S., Obrietan, K. & Storm, D. R. (1999) *Neuron* **23,** 11–14.
32. Barria, A., Muller, D., Derkach, V., Griffith, L. C. & Soderling, T. R. (1997) *Science* **276,** 2042–2045.
33. Derkach, V., Barria, A. & Soderling, T. R. (1999) *Proc. Natl. Acad. Sci. USA* **96,** 3269–3274.